SLAC–PUB–6610
August 1994
(A)

NEXT LINEAR COLLIDER TEST ACCELERATOR INJECTOR DESIGN AND STATUS*

A. D. Yeremian, R. H. Miller, and J. W. Wang
Stanford Linear Accelerator Center, Stanford University, Stanford, CA 94309, USA

Abstract

The Next Linear Collider Test Accelerator (NLCTA) being built at SLAC will integrate the new technologies of X-band accelerator structures and RF systems for the Next Linear Collider, demonstrate multibunch beam-loading energy compensation and suppression of higher-order deflecting modes, measure transverse components of the accelerating field, and measure the dark current generated by RF field emission in the accelerator [1]. Injector design and simulation results for the NLCTA injector are discussed.

Introduction

The NLCTA injector is simple, reliable, and capable of delivering the average beam required for the various beam loading and acceleration tests for the X-band accelerator structures for the NLC. The injector consists of a thermionic gun, two X-band prebunchers, a 0.9 m buncher/capture accelerator section, and a second 0.9 m accelerator section (see Fig. 1). Immediately following the injector is a straight section of beam line consisting of quadrupoles and X and Y variable collimators, followed by a chicane with an energy spread defining collimator in the high dispersion section. Following this is the accelerator, consisting of standard 1.8 m X-band sections to be tested for the NLC. There are 34 solenoidal magnets from the gun to the end of the second 0.9 m accelerator section for controlling the transverse dimension of the beam.

The goal of the NLCTA injector is to deliver to the accelerator a pulsed beam variable in length from 5 to 140 ns consisting of a train of microbunches 1.3 ps in length, 87.5 ps apart, with 0.4×10^{9} electrons per microbunch; that is 0.75 A average current. The RMS energy spread should be less than 0.5% and the RMS normalized emittance less than 5×10^{-5} m-rad. Allowing ourselves margin for error, we chose to deliver 1.5 A average current to the accelerator section. The gun is capable of producing 6.2 A at 150 KeV; the simulations were done for a gun current of 4.5 A at 150 KeV.

We used the beam parameters at the anode calculated by EGUN and the space harmonic amplitudes for the electric fields in the RF cavities calculated by SUPERFISH as input to PARMELA to simulate the injector from the gun to the first quadrupole at the end of the injector. The rest of the accelerator was designed using transport and is not the subject of this paper.

Gun Design

The thermionic gun is similar to the one on the Stanford Linear Collider (SLC) injector, and uses a 2 cm^2 grided circular cathode pulsed at 10 Hz with a square pulse variable from 5 to 140 ns.

EGUN was used to design the thermionic gun focus and anode electrode shape, and the gap between them, and to simu-late the beam parameters in the gun region. While the focus and anode electrode shapes are unchanged from the SLC gun configuration, the anode cathode gap is modified to achieve the best emittance for a space charge limited flow of 4.5 A at 120 KeV; with an operating goal of 4.5 A and 150 KeV. The anode cathode gap distance is 47 mm and the perveance is 0.11 μperv. Simulations include the thermal energies assum-ing the cathode will be heated to 950˚C. Space charge limited flow at 150 KeV is 6.2 A. Figure 2 shows the beam envelope for the intended gun operation of 150 KeV and 4.5 A. The normalized edge emittance for this case is 9.5 π-mm-mrad and the beam radius at the waist near the anode is 5 mm.

Bunching and Beam Transport System

Solenoidal magnets from the gun to the end of the second 0.9 m accelerator for the injector were simulated using single coils in PARMELA. Thirty-one out of the 34

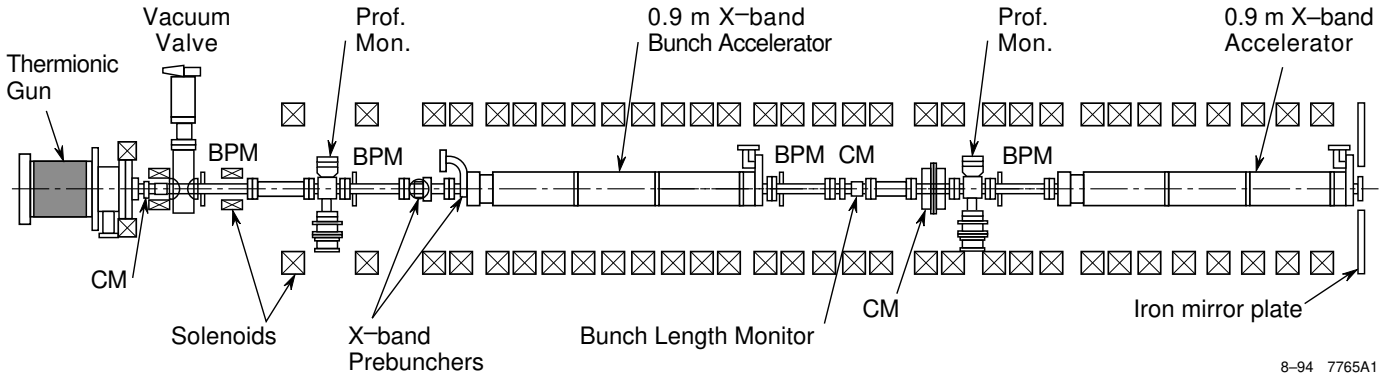

Fig. 1. The NLCTA Injector layout.

*Work supported by Department of Energy contract DE–AC03–76SF00515

Presented at the 17th International Linear Accelerator Conference (LINAC 94), Tsukuba, Japan, August 21–26, 1994

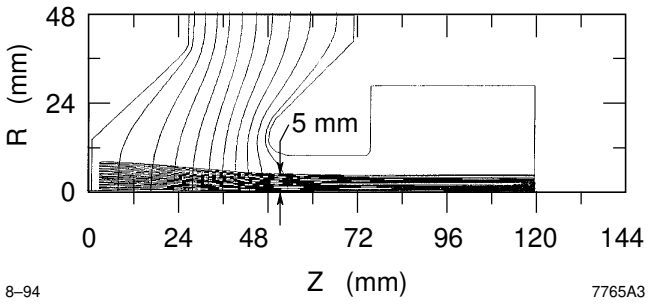

Fig. 2. Beam envelope from the NLCTA thermionic gun.

solenoids in the injector are large, with an inner radius of 21 cm and outer radius of 28 cm, distributed as shown in Fig. 1. Two of the solenoids are small lenses near the gun, and are used for matching the beam from the gun into the large solenoid area. One solenoid is used very near the cathode as a bucking coil to reduce the axial magnetic field at the cathode to zero. No iron is used anywhere in the injector, except for the iron mirror plate at the very end of the second accelerator section, to prevent the solenoidal magnetic field from penetrating into the quadrupole region. The axial magnetic field (Fig. 3) varies from 0 G at the cathode to about 3800 G at the entrance to and over the first accelerator section. The edge radius of the beam in the first and second accelerator sections is less than one half of the r = 0.4 cm aperture in these sections, while the RMS beam radius is only about 0.03 cm as shown in Fig. 4. The magnetic field in the drift region between the two accelerator sections and over the second accelerator is chosen so that the beam leaving the second accelerator is convergent.

The bunching system consists of 2 X-band prebunchers and a traveling wave tapered phase velocity buncher accelerator section. SUPERFISH [3] was used to simulate the electric fields in the X-band prebunchers, buncher, and accelerator sections. The Fourier coefficients of the bunchers along with the beam parameters from the gun were used as input in the PARMELA code to optimize buncher amplitude, phase, and separation for optimum bunching, and the solenoidal magnets were optimized for controlling the beam transverse size. The two standing wave prebunchers require 8 and 30 KV respectively for optimum bunching, and are separated by about 15 cm. The distance between the second prebuncher and the buncher is only about 5 cm because the beam tends to debunch due to space charge for drifts longer than 5 cm. The microbunch peak current is 15 A and the energy is 153 ± 25 KeV at the entrance to the buncher.

For maximum bunching, we found that the cavities in the first accelerator section need to start at a phase velocity of less than the speed of light and gradually taper up to the speed of light. The X-band buncher/accelerator section consists of 105 cells, where the first three cavities have a phase velocity of 0.6c, 0.7c, and 0.9c, respectively, and the rest a phase velocity of c. The gradient in the first four buncher cavities is 35, 38, 46, and 50 MV/m, respectively. From here, it tapers down linearly to 41 MV/m by the end of the first accelerator section due to beam loading. The bunching process is complete by the time the beam travels through the tenth cell of the buncher/accelerator section, and the beam slips to 6° ahead of the crest by the time it exits the section with $E = 40.9 \pm 0.1$ MeV. The second accelerator section is 0.9 m long with independent phase and amplitude shifters, allowing us to accelerate the beam on the crest of the RF. All the cavities have a phase velocity of c, and the gradient tapers from 50 to 41 MV/m along the section due to beam loading. The beam exits this section with $E = 82.9 \pm 0.15$ MeV.

Figure 5 shows the beam parameters at the end of the second accelerator section as calculated by PARMELA. Micro-bunch width at the end of the injector is about 5° of X-band FWHM and 73% of the initial charge at the gun is captured in 15°. The particles outside the main 15° pulse,

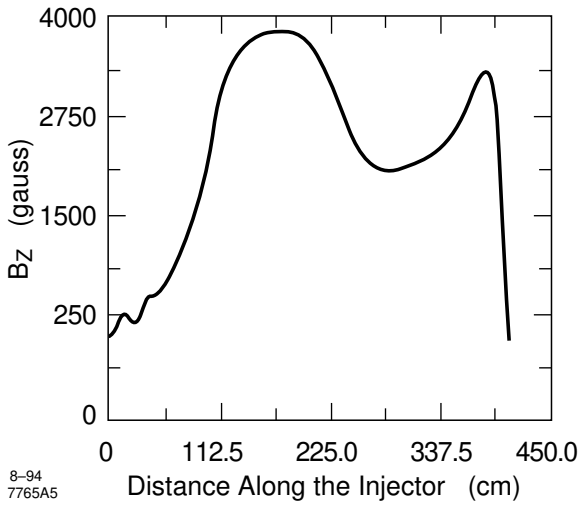

Fig. 3. Axial magnetic field along the NLCTA injector.

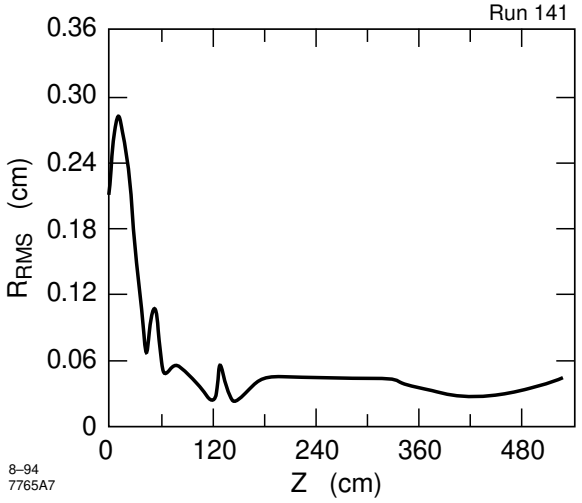

Fig. 4 Electron beam RMS radius along the NLCTA injector.

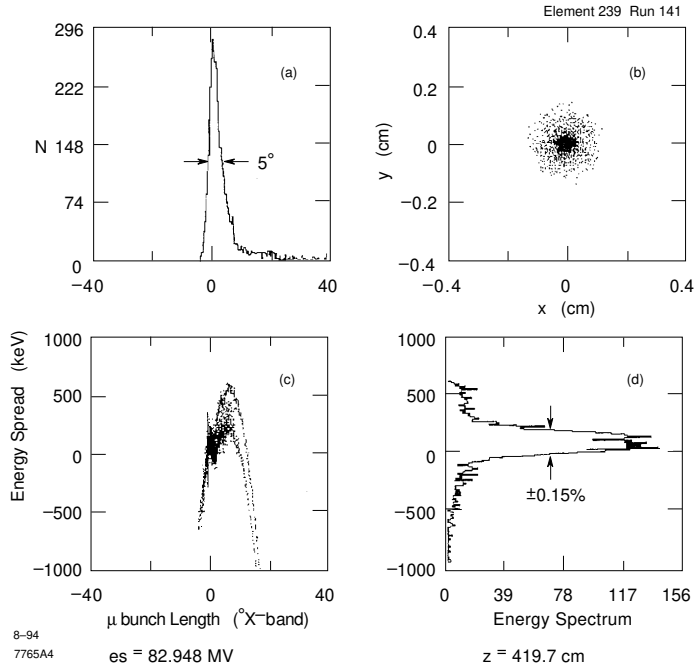

Fig. 5. Electron beam parameters at the end of the NLCTA injector: (a) the microbunch pulse shape, (b) the transverse and (c) the longitudinal beam distribution, and (d) the energy spread profile.

almost entirely contained in the low-energy tail, can be scraped away with the collimators in the high-dispersion area of the chicane, allowing us to accelerate 3.3 A of average macropulse current with a clean micropulse structure that does not exceed 15°. Normal-ized RMS emittance of the beam at the exit of the injector is about 1×10^{-5} m-rad and can be reduced to 6×10^{-6} m-rad if we use the X and Y collimators right after the injector to scrape away the radial halo (see Fig. 4b) of the beam. About 12% of the charge is contained in this halo.

If we choose to use all three collimators available to us, and scrape away both the halo and the high-energy tail of the beam, then we can expect a 2.8 A macropulse current with a normalized RMS emittance of 6×10^{-6} m-rad at the end of the chicane going into the first 1.8 m NLC type accelerator section. Table 1 compares the NLCTA requirements with simulated achievable results, with and without collimation.

TABLE 1

Electron Beam Requirements and Simulation Results for the NLCTA Injector

Parameter	Requirement	Simulation	
		Collimation	
		No	*Yes*
Total transmission gun to end of injector	---	0.84	0.64
Capture in 15° X--band (%)	—	74	63
I_A due to charge in 15° X--band (A)	1.5	3.3	2.8
Charge / μbunch (nc)	0.1	0.3	0.25
μbunch width FWHM (degrees °X-band)	10	5	5
ε_{nrms} (m-rad)	$< 5\times10^{-5}$	1×10^{-5}	6×10^{-6}
ΔE/E FWHM (%)	< 0.5	0.3	0.3

Conclusion

Single-bunch simulations show that the microbunch beam requirements for the NLCTA accelerator can be reached with a simple injector consisting of all X-band bunching compo-nents. Beam-loading effect studies, which include phase shifts in the bunching components, are currently under study and seem to present no obstacles that cannot be overcome by careful choice of hardware parameters. These studies will be summarized in another paper at a later date.

Many of the injector components already exist or are on order. It is our goal to commission the injector with beam in the summer of 1995.

Reference

1. NLC Test Accelerator Conceptual Design Report, SLAC Report-–411, August 1993.